Mon. Not. R. Astron. Soc. **000**, 1–9 (2003) Printed 2 February 2008 (MN LATEX style file v2.2)

Radio-optical flux behavior and spectral energy distribution of the intermediate blazar GC 0109+224

Stefano Ciprini[1,2⋆], Gino Tosti[1,2], Harri Teräsranta[3], and Hugh D. Aller[4]
[1] *Physics Department and Astronomical Observatory, University of Perugia, via Pascoli, 06123 Perugia, Italy*
[2] *INFN Perugia Section, via Pascoli, 06123 Perugia, Italy*
[3] *Metsähovi Radio Observatory, Helsinki University of Technology, 02540, Kylmälä, Finland*
[4] *Department of Astronomy, Dennison Bldg., University of Michigan, Ann Arbor, MI 48109, USA*

submitted to MNRAS

ABSTRACT

About twenty years of radio observations in five bands (from 4.8 to 37 GHz) of the BL Lac object GC 0109+224 (S2 0109+22, RGB J0112+227), are presented and analysed together with the optical data. Over the past ten years this blazar has exhibited enhanced activity. There is only weak correlation between radio and optical flares delays, usually protracted on longer timescales in the radio with respect to the optical. In some cases no radio flare counterpart was observed for the optical outbursts. The radio variability, characterised by peaks superposition, shows hints of some characteristic timescales (around the 3-4 years), and a fluctuation mode between the flickering and the shot noise. The reconstructed spectral energy distribution, poorly monitored at high energies, is preliminarily parameterised with a synchrotron-self Compton description. The smooth synchrotron continuum, peaked in the near-IR-optical bands, strengthens the hypothesis that this source could be an intermediate blazar. Moreover the intense flux in millimetre bands, and the optical and X-ray brightness, might suggest a possible detectable gamma-ray emission.

Key words: BL Lacertae objects: general — BL Lacertae objects: individual (0109+224) — BL Lacertae objects: individual (0112+227) — methods: statistical — radiation mechanisms: nonthermal — blazars

1 INTRODUCTION

The compact radio–loud source GC 0109+224 (S2 0109+22, TXS 0109+224, RX J0112.0+2244, EF B0109+2228, RGB J0112+227), belonging to the Green Bank radio survey list C, is a synchrotron source known for more than thirty years (Pauliny-Toth et al. 1972) and was optically identified few years later (Owen & Mufson 1977). It is a strong radio-millimetre active galactic nucleus (AGN), with variable flux, polarisation degree and position angle, showing a flat average spectrum much like the classical BL Lac objects. Unfortunately it is poorly studied beyond optical frequencies. The milliarcsecond (pc) scale of GC 0109+224 reveals a compact core, and a secondary component with no additional diffuse emission, and less luminous and/or beamed than the 1-Jy sample sources (Bondi et al. 2001; Fey & Charlot 2000). The kpc scale shows a faint one–sided collimated radio jet, about 2 arcsec long (Wilkinson et al. 1998), largely misaligned with the pc-scale inner region, as is frequently observed in high-luminosity and low-energy peaked BL Lac objects (LBLs, with the peak in infrared bands). This source is a member of the 200-mJy catalog (Marchã et al. 1996), a sample which seems to fill the gap between the high energy peaked BL Lacs (HBLs, with the peak in the UV, soft-X bands) and the LBLs, as expected by some current blazar unification pictures.

The historical optical light curve shows a behavior intermediate between the larger–amplitude variable BL Lacs, and the smaller–amplitude variable flat spectrum radio quasar (FSRQs). Increased flare activity (rapid optical variations, peak superposition, rapid flux drops), is clearly shown after 1994 in the optical bands, thanks to the increased data sampling of the Perugia University Observatory, which has also recorded the larger and faster flares (Ciprini et al. 2003a). During seven years GC 0109+224 showed six main optical outbursts (weeks/month scale), and a variability mode placed between the flickering and the shot noise.

Rather achromatic long term optical behaviour , is accompanied by isolated outbursts with loop–like hysteresis of the spectral index, indicating that rapid optical variability is dominated by non-thermal cooling of a single electron population (Ciprini et al. 2003a). Both the optical flux

⋆ offprints: stefano.ciprini@pg.infn.it

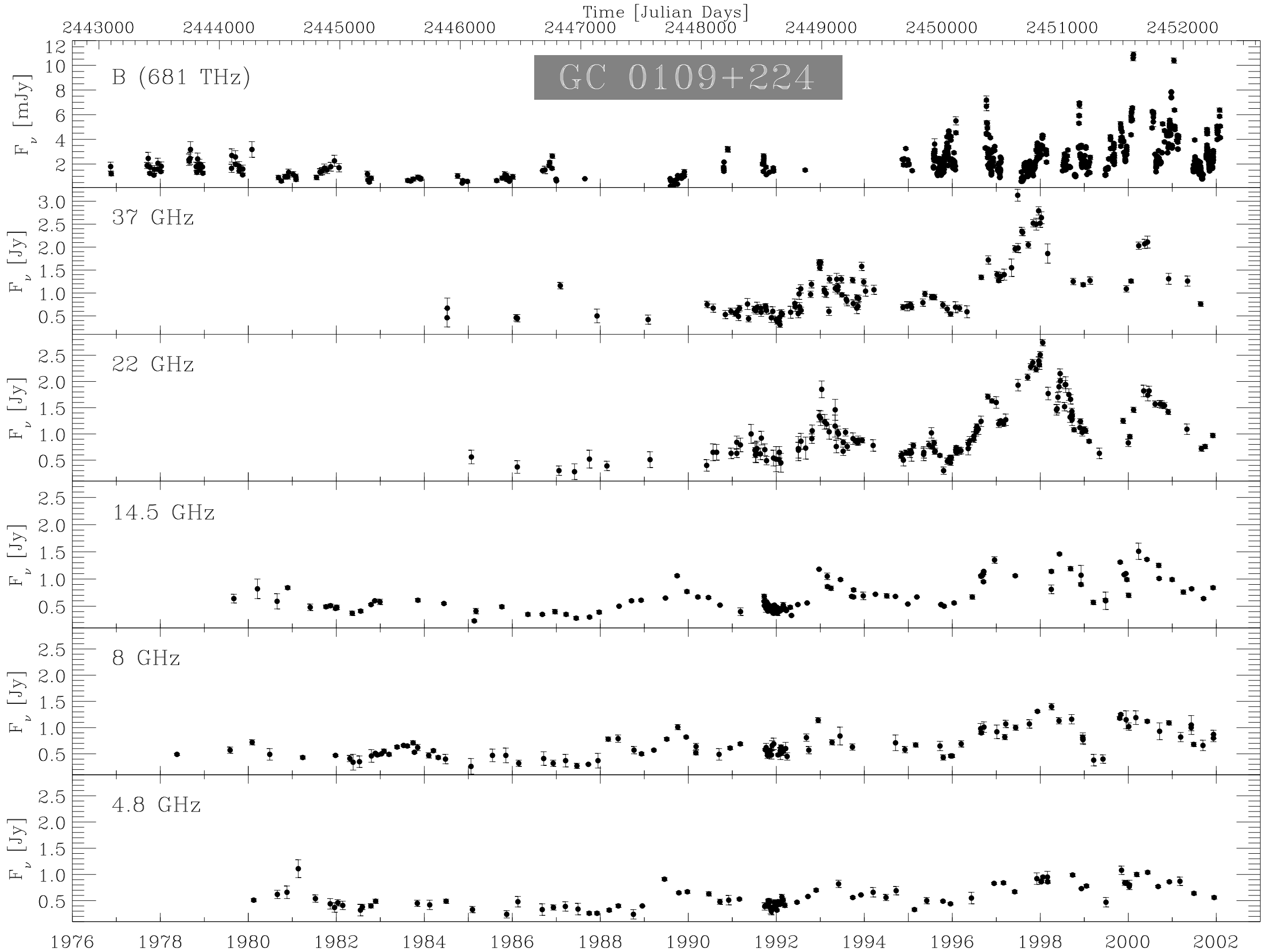

Figure 1. The complete radio–optical density flux light curves of GC 0109+224. The optical observations are historical, and Perugia Obs. (Italy) data (the post-1994 data points), reported in the original or extrapolated Johnson B band (see for details Ciprini et al. 2003a). The high sampled data at 37 and 22 GHz are from Metsähovi (Finland), and the 14.5 GHz, 8 GHz, 4.8 GHz data are from the long term monitoring of the UMRAO, (USA). This source clearly exhibit a higher mean–flux level, and an enhanced activity in the radio–mm after 1992, and in the optical after 1994, even if the optical sampling before this year is insufficient to record faster (and usually larger) flares.

and the polarization are known to be variable on different timescales, including intraday variability (Sitko et al. 1985; Mead et al. 1990; Valtaoja et al. 1991). The relatively strong variable degree (up to 30%) and direction of the optical linear polarisation, is one of the most noticeable characteristics of this object (Takalo 1991; Valtaoja et al. 1993), even if there is no clear correlation between the flux level and polarisation degree. The host galaxy of GC 0109+224 is still unresolved (Falomo 1996; Wright et al. 1998), but a lower limit to the redshift $z \geqslant 0.4$ is suggested (Falomo 1996). From the old IRAS data there is no evidence for a thermal component in the far–infrared (Impey & Neugebauer 1988).

GC 0109+224 was detected in the past at X-ray bands by satellites *Einstein*, EXOSAT, ROSAT, and the source is a member of the RGB catalog (Laurent-Muehleisen et al. 1999), a list of intermediate blazars with properties smoothly distributed in a large range between the LBL and HBL subclasses. In the diagnostic diagram α_{ro}-α_{oX} (Padovani & Giommi 1995), GC 0109+224 appears close (Dennett-Thorpe et al. 2000) to a prototype of intermediate blazars like ON 231 (W Com, Tosti et al. 2002; Böttcher et al. 2002; Tagliaferri et al. 2000). The HBL and LBL subclasses exhibit systematically distinct properties (i.e. F_X/F_{rad} flux densities ratio, degree of radio core dominance, optical polarization degree and variability, etc.). The so called "intermediate" blazars are critical to clarify the relationship between these subclasses, and to validate the unified schemes based on bolometric power. Intermediate blazars often peak in optical bands (thus are selected and monitored mainly by optical telescopes), and during some variability phases the break between the two overall spectral components occurs in the X-ray bands. In some cases their spectral energy distributions (SEDs) can be still described well with synchrotron-self-Compton (SSC) models (like for the HBLs), and this implies, by simple scaling arguments, a possible inverse Compton (IC) emission peaked in GeV gamma-ray bands (see, e.g. Stecker et al. 1996). In the case of GC 0109+224 EGRET did not detected any gamma-ray emission (phase 1, Fichtel et al. 1994), with a rather low upper limit of 0.01 nJy above 100 MeV.

GC 0109+224 is regularly monitored by the Univer-

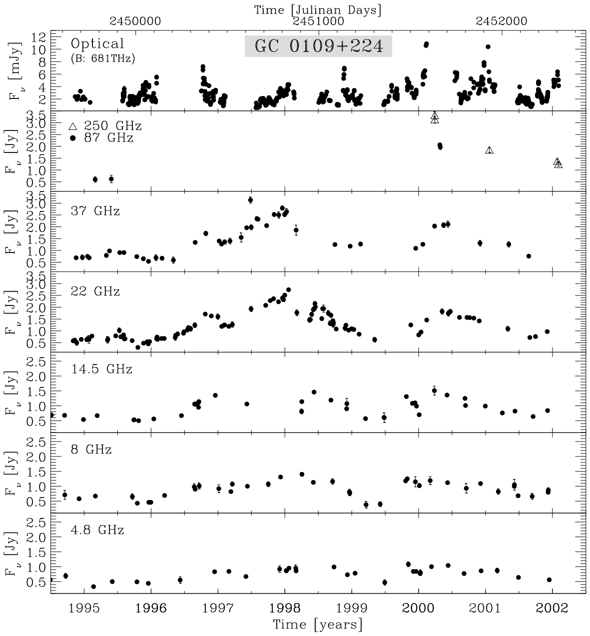

Figure 2. The post-1994 portion of the flux curves in Fig. 1, that match the optically best sampled period. A few observations at mm wavelength (87 and 250 GHz) are also added in this plot. In this detail radio flares clearly appear to work on considerably longer timescales, with respect to the optical flares. The relevant emission bump between the end of 1995 and mid–1999 (clearly visible in the 22 GHz curve), seems to be the result either of superposition of four flares departing from base level, or superposition of four peaks departing from a slower base level bump. Noteworthy is also the February-April 2000 outburst, because it seems detected (during the last decreasing phase) at all seven mm–radio frequencies reported in this plot.

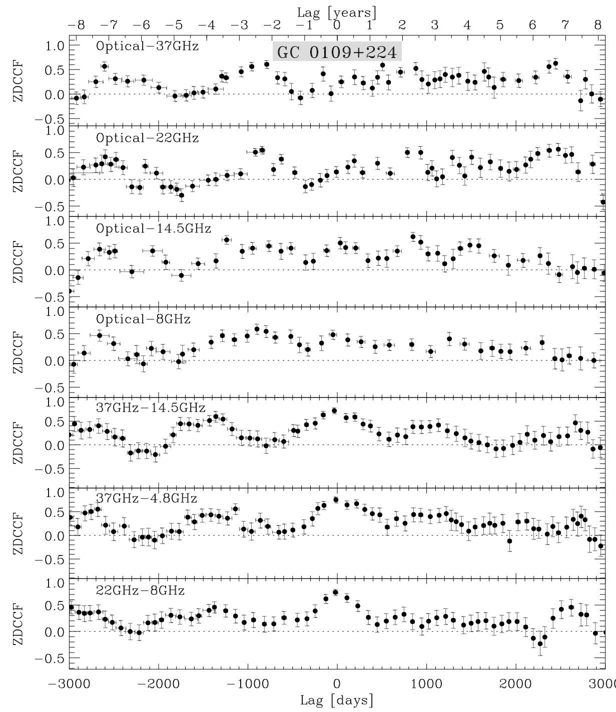

Figure 3. Cross correlation calculated with the z-transformed discrete correlation function (ZDCF, Alexander 1997). Due to the different timescales for the duty cycles in the radio and optical, and to gaps empty of data in the optical, no strong evidence of a radio–optical correlation is found. Weak peaks in the cross–correlations (ZDCCF coefficient $\simeq 0.5-0.6$) are found around a lag of 900 days (also positive in the optical–22GHz correlations, see text). On the other hand, the fluxes at the various radio frequencies appear well correlated, as expected, with a peak around the zero lag.

sity of Michigan Radio Astronomy Observatory (UMRAO), USA (see, e.g. Aller et al. 1996) and by the Metsähovi Radio Observatory, Finland (see, e.g. Teräsranta et al. 1998). In order to search for time correlations between the optical and radio fluctuations at the various bands, in Section 2 the updated radio flux data of UMRAO and Metsähovi are compared with the available optical data (reported in Ciprini et al. 2003a). In Section 3 the temporal behavior of the radio light curves is investigated through well known methods suitable for unevenly data sets. In Section 4 we show the reconstruction of the SED, with the available multiwavelength data, and a first estimation of the bolometric energy and physical parameters using a pure SSC model.

2 RADIO-OPTICAL CORRELATIONS

The reconstructed optical flux history of GC 0109+224, and the last seven years of data collected mainly during the Perugia monitoring program, are compared with the updated radio flux observations, belong to the Metsähovi (37 GHz and 22 GHz data), and UMRAO (14.5 Ghz, 8 Ghz and 4.8 GHz data) radio observatories. At centimetre and millimetre bands (up to about 90 GHz) a monthly sampling for blazars is in most cases enough. The source was monitored at an appreciable rate especially at 22 GHz, and in a significant long-term period at 4.8, 8 and 14.5 GHz. Some essential properties of the centimetre emission of this blazar measured at UMRAO are outlined in (Aller et al. 1999). Metsähovi data up to 1998 were compared with few literature optical observations (only 1996-1998), finding a lag of about 400 days between optical and 22 GHz variations (Hanski et al. 2002).

The complete optical (Johnson B band) and radio light curves of GC 0109+224, are plotted in Fig. 1. Increased activity was observed after 1992 in all five radio bands. Available optical data are too few prior to 1995, to check the beginning of enhanced emission at this band. Since 1995 Perugia observations have increased the sampling density, recording also the larger (and faster) flares, showing well increased activity, rapid variations, and the same flares superposition which seems to characterise the radio flux. The flux history of the source, with millimetre data added, is plotted in Fig. 2 in more detail. Radio outbursts are clearly longer then the optical one, and show smaller amplitudes at lower frequencies. The peak frequency, in which the highest flux is observed during the flare, seems, at least for the outburst of March-April 2000 (2000.4, Fig. 2), to be around millimetre wavelengths (as an intense flux of 3.13 ± 0.04 and 3.31 ± 0.06 Jy at 250 GHz, was detected by the Mambo bolometer at IRAM on 29 March 2000, Bertoldi 2002).

The 22 and 37 GHz curves of Fig. 2, show the faster features in the radio, and five main peaks: around 1996.7 (visible also at 14.5, 8 and 4.8 GHz), around 1997.5, another

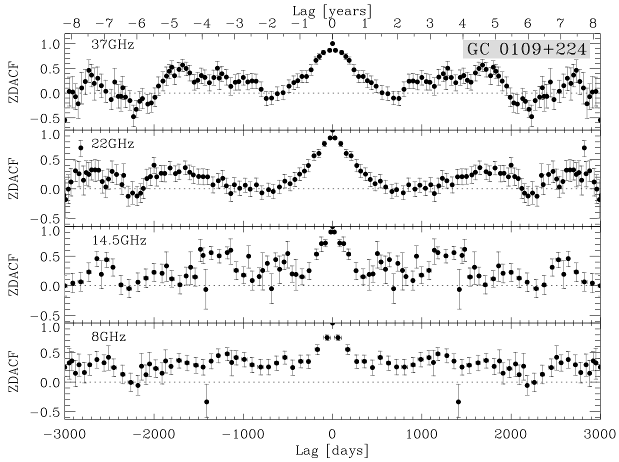

Figure 4. The auto–correlations of the radio flux curves, calculated with the ZDCF. These do not show any relevant feature, except for broad and weak ($ZDACF \simeq 0.6$) peaks around the timescale of 3.14-4.06 years (at 14.5 GHz), and around 3.53-4.60 years (at 37 GHz). From 37 GHz to 14.5 GHz, the ZDACF profile resemble to a shot noise, with a single bump in the correlation curve within the 2000 days timescale (semi–amplitude $\simeq 2.7$ years).

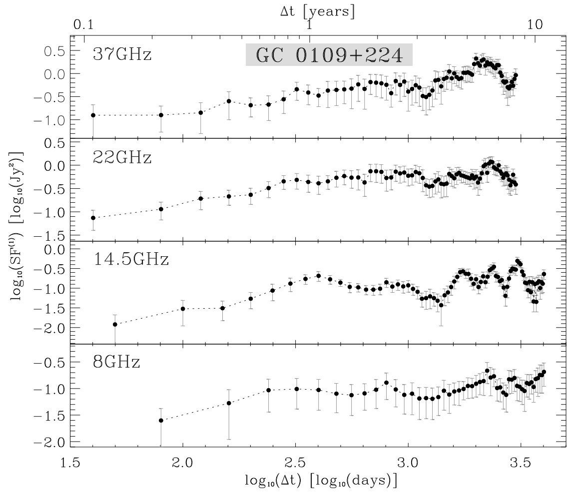

Figure 5. The first order structure functions (SF) of the radio density flux light curves, in logarithmic scale. For the 37 GHz flux curve, the mean slope index of the steep part of the SF is $\beta = 0.48 \pm 0.08$, and for the 22 GHz curve $\beta = 0.65 \pm 0.05$ (bin size used is 40 days for both). For the 14.5 GHz series the SF mean slope is $\beta = 0.39 \pm 0.14$, and for the 8 GHz data $\beta = 0.52 \pm 0.13$, (50 days the bin size used). The time scales corresponding to deepest drops in the SF are of 3.4-3.8 and 7.4-7.6 years. The shorter lags at which there are hints of a flattening in the curves, are around 1.1-1.8 years.

around 1998.0 (seen also at 8 GHz), still one before 1998.5 (seen also at 14.5 GHz, while the 37 GHz receiver was down), and another around 2000.4 (this is seen in all the bands). Other peaks are easily identifiable (Fig. 1) around 1993.0 (from 8 GHz to 37 GHz), and at the end of 1989 (from 4.8 GHz to 14.5 GHz). The more violent optical activity in these years (Fig. 2) is characterised by six main flares of much shorter duration (on the order of weeks-one month), with faster rise and decline.

The noticeable temporal structure in the radio flux curves, between the end of 1995 and mid–1999, looks like an underling emission bump spreading over 3.5 years, with four superposed main peaks, or a superposition of four flares departing from the base level. It's difficult, even visually, to link this radio bump to a specific optical peak. The optical emission in this period, apart of an outburst in Oct. 1996, decreases to a ground level, with a few flickering low peaks until mid–1997, then rises almost monotonically with a flickering behaviour, up to beginning of 1998, and then displays another relevant flare only during November 1998 (Ciprini et al. 2003a). Another prominent radio outburst occurred in February-April 2000, and seems detected at all the seven mm-radio frequencies (from 4.8 to 250 GHz, Fig. 2), during the final slow decreasing phase.

Blazars usually exhibit shorter variability timescales, and more numerous flares in the optical, than in mm-radio bands, and the optical data are often heavily affected by empty gaps in the observations (seasonal interruptions, and weather conditions). This is a problem in the search of correlations. The level of correlation can be investigated with the Discrete Correlation Function (DCF, Edelson & Krolik 1988; Hufnagel & Bregman 1992), and the Interpolated Correlation Function (ICF, Gaskell & Peterson 1987), suitable for discrete unevenly sampled data sets. In the DCF the number of point per time bin can vary greatly, in the ICF instead, the interpolation may be unreliable if the curves are under-sampled. We applied a method that is more robust especially when the data are few, ensuring that there is a statistically meaningful number of points in each bin: the Fisher z-transformed DCF, (ZDCF, Alexander 1997). This method build data bins by equal population rather than equal width, and uses Montecarlo estimations for peaks and uncertainties.

For a lag between 789 and 879 days (2.1-2.4 years), no peaks with large values were found in the optical–radio cross correlation curves (ZDCCF values from 0.50 to 0.62, Fig. 3). Other shorter radio-optical delays for which ZDCCF peaks are recognizable, are around the delay of 190 days (observed in both the correlations with the 37 and 22 GHz fluxes, but it is not meaningful because $ZDCCF \simeq 0.35$), around a lag of 33 days ($ZDCCF \simeq 0.50$) between optical-14.5 GHz curves, and around a lag of about 500 days ($ZDCCF \simeq 0.59$) between optical-37 GHz fluxes. Interesting to note is that the cross–correlations, with a peak around the 2.1-2.4 years lag range (both positives, delays, and negatives, leads), are found in all the optical–radio (37, 22, 14.5 and 8 GHz) correlation curves, (Fig. 3). This also appears when applying the standard DCF method. Hints of optical–radio correlation around this lag timescale, is also present in the plots of (Hanski et al. 2002), while the 350 and 400 days lags cited in this work (based only on two years of optical data), was not confirmed by our data.

The optical–radio delays found around 2.1-2.4 years, do not represent strong evidence for a real physical correlation, because the timescales suggested are very long. Even though the coefficients are not low (0.5-0.6) and the correlations are found for all radio frequencies correlations. On the other hand shorter delays around 33, 190, 500 days are not significant, because they are found with low value correlations coefficients. To investigate better the radio–optical delays, it is necessary to increase data sampling in future optical monitoring programs.

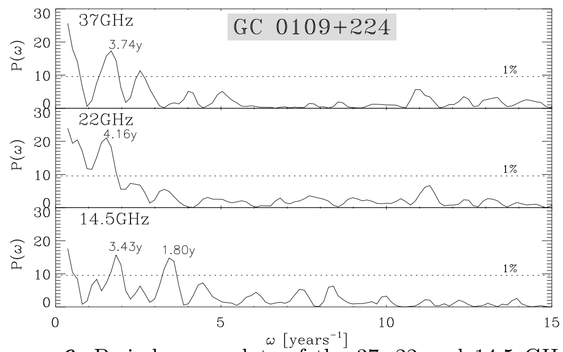

Figure 6. Periodogram plots of the 37, 22 and 14.5 GHz flux curves. Dotted lines shows the 1% false alarm significance level, under the hypothesis of fluctuations dominated by Poisson statistics. The timescales corresponding to the peaks above this level, are 1.80, 3.43, 3.74 and 4.16 years.

3 RADIO FLUX VARIABILITY

The radio flux auto–correlation curves (ZDACF and DACF) of GC 0109+224 in various bands (Fig. 4), do not show very relevant feature, except for broad and weak ($ZDACF \simeq 0.6$) peaks around the scale of 3.14-4.06 years in the 14.5 GHz curve, and around 3.53-4.60 years in the 37 GHz curve. From 37 GHz to 14.5 GHz the auto–correlation profile resembles shot noise, with a single bump in the correlation curve of semi–amplitude $\simeq 2.7$ years.

In Fig. 5 we plotted the first order structure functions (SFs) (e.g. Simonetti et al. 1985; Hughes et al. 1992) of the radio light curves. The SF works in the time domain instead of frequencies f. It measures of the mean difference in the data train as a function of the separation time Δt in the sampling. In log–log plots the SF of an ideal time series plus measurement noise, increases and shows an intermediate steep curve ($SF(\Delta t) \propto (\Delta t)^{\beta}$). The slope β depends on the nature of the intrinsic variability, and give the Fourier power law index of the spectrum, (say $P(f) \propto 1/f^{\beta+1}$, where f is the frequency). The values of β for GC 0109+224 (Fig5), go from 0.39±0.16 to 0.65±0.08, meaning an intermediate variability mode, between the pure flickering (pink noise, $\beta = 0$) and the shot noise (red/brown noise, $\beta = 1$). Deep and steep drops in the SF plots means a little variance, and then a possible signature of characteristic time scales: it is apparent at about 3.4-3.8 years and 7.4-7.6 years. Other characteristic timescales are given by the turnover lag where the SF profile begin to flatten, and in the plots of Fig. 5 these are located around 1.1-1.8 years, even if in our data the flattening is recognizable only with difficulties.

In Fig. 6 are reported the Lomb–Scargle periodograms (Scargle 1982; Horne & Baliunas 1986) of the radio curves which present some features. This technique (calculated with a fast algorithm Press & Rybicki 1989), analogous to the Fourier analysis for unevenly sampled data sets, useful to detect possible periodicity, and typical timescales. The components above the 1% false alarm threshold, annotated in Fig. 6 (from 1.8 to 4.16 years), are not very significant, and not easily visually identifiable in the flux light curves.

The length of the data record, required to demonstrate a real recurrent timescale depends on signal–to–noise ratio, systematic errors, regularity in sampling, nature of the measurements, and the nature of the underlying variation. Even if the strength of the autocorrelations found is not high, from the beginning of 1990s our radio sampling is sufficient at all the five bands observed to consider this discovered hints of timescales, a starting point in the search for recurrent times with future observstions. As mentioned above, hints of a sort of periodicity (or at least of a typical timescale) around 3-4 years, are found by applying all three methods. Future radio flux data, with increased sampling and extended observing period, and VLBI observations may or may not confirm this timescale.

Table 1. Some roperties and fluxes of GC 0109+224. (1) optical counterpart *Hipparcos* coordinates (Zacharias et al. 1999); (2) redshift lower limit (Falomo 1996); (3) 82 cm flux density (Douglas et al. 1996); (4) 20 cm flux density (Owen et al. 1980); (5) mean flux densities from this work; (6) 87 GHz flux from Metsähovi; (7) 1.2 mm Mambo-IRAM detection (Bertoldi 2002), (8) IRAS far-IR flux at 60 μm (Impey & Neugebauer 1988); (9) mid-IR flux in L band (Odell et al. 1978); (10) mean optical flux in R Cousins band (Ciprini et al. 2003a); (11) mean optical flux in B Johnson band from historical light curve (Ciprini et al. 2003a); (12) optical (B band) min and max degree of liner polarization (Valtaoja et al. 1993; Takalo 1991); (13) X-ray flux at 2 keV by Einstein Observatory (HEAO-2) IPC and MPC instruments (Owen et al. 1981; Ledden & Odell 1985; Maraschi et al. 1986); (14) X-ray flux at 1 keV by CMA instrument on EXOSAT (Maraschi & Maccagni 1988; Giommi et al. 1990; Reynolds et al. 1999); (15) X-ray flux at 1 keV by PSPC instrument of ROSAT (Neumann et al. 1994; Brinkmann et al. 1995; Reich et al. 2000) and spectral index (Kock et al. 1996; Laurent-Muehleisen et al. 1999); (16) flux limit above 100 MeV by EGRET (see Tab. 2), (Fichtel et al. 1994).

Quantity	Value	Epoch	Ref.
R.A.(J2000.0)$_{opt}$	01h 12m 05.8238s	...	(1)
Dec.(J2000.0)$_{opt}$	+22° 44' 38.798"	...	(1)
z	> 0.4	...	(2)
F_ν(0.365 GHz)	0.279 ± 0.021 Jy	...	(3)
F_ν(1.484 GHz)	0.36 ± 0.2 Jy	Jan78	(4)
$<F_\nu$(4.8 GHz)$>$	0.56 Jy	Feb80-Dec01	(5)
$<F_\nu$(8 GHz)$>$	0.67 Jy	May78-Dec01	(5)
$<F_\nu$(14.5 GHz)$>$	0.66 Jy	Sep79-Dec01	(5)
$<F_\nu$(22 GHz)$>$	1.07 Jy	Jan85-Dec01	(5)
$<F_\nu$(37 GHz)$>$	1.05 Jy	Jul84-Aug01	(5)
F_ν(87 GHz)	2.06 ± 0.09 Jy	2000 Apr 26	(6)
F_ν(250 GHz)	3.31 ± 0.06 Jy	2000 Mar 29	(7)
F_ν(60 μm)	188 mJy	1983	(8)
F_ν(3.5 μm)	11.8 mJy	Jan77	(9)
$<F_\nu$(0.64 μm)$>$	3.8 ± 0.2	Nov94-Feb02	(10)
$<F_\nu$(0.44 μm)$>$	2.4 ± 0.3	Nov76-Feb02	(11)
P(B)$_{min/max}$	0.7% / 29.69 %	...	(12)
F_ν(2 keV)	0.15 μJy	Jul 1979	(13)
F_ν(1 keV)	0.21 μJy	Aug 1984	(14)
F_ν(1 keV)	0.26 ± 0.08 μJy	Aug 1990	(15)
α_X	1.96 ± 0.25	Aug 1990	(15)
F_ν(> 100 MeV)	< 0.01 nJy	1992	(16)

4 THE SPECTRAL ENERGY DISTRIBUTION

GC 0109+224 is a bright X-ray point source ($\nu F_\nu(1 \text{ keV}) \gtrsim 10^{-13}$ erg cm^{-2} s^{-1}), known since the observation of HEAO-1 A2 experiment (Della Ceca et al. 1990) in Jan. 1978. The spectral energy distribution (SED) assembled with the available historical multiwavelength data, is shown in Fig. 7 (references for data in figure's caption), and is compatible with a smooth continuum given by a pure synchrotron component, like the classical BL Lac objects. In

Table 2. EGRET viewing periods (v.p.) and flux upper limits (u.l.) of GC 0109+224. Related quasi-simultaneous radio and optical fluxes from this work, are also reported in the Table when available. References: (a) EGRET integral flux density upper limit above 100 MeV (first EGRET catalog, phase 1) for three v.p. (Fichtel et al. 1994); (b) the only simultaneous optical data available (Valtaoja et al. 1993), points out a low brightness and polarization degree 5.20 ± 0.61; (c) u.l. given by the summed exposures of phase 1 pointings, and the other EGRET v.p. of the GC 0109+224 region on phase 3 and cycle 4 (1994-95) (Hartman et al. 1999). Any new pointing of the region was done during the EGRET phase 2 (Nov.1992-Sept.1993, Thompson et al. 1995). During EGRET cycle 8, at least one more pointing was available (2000, Apr.18-Apr.25) but our source was on the edge of the field of view. Throughout all the EGRET v.p. the source had a relatively low (sub-Jy) radio emission.

EGRET v.p.	Start-End Date	$F_\gamma(> 100\mathrm{MeV})$ [ph cm^{-2} s^{-1}]	Ref.	Optical obs. epoch	F_{opt} [mJy]	Ref.	Radio obs. epoch	F_{rad} [Jy]
0260....	1992 Apr 23 - Apr 28			...	...		1992 Apr 26	$F_{14.5} = 0.48 \pm 0.03$
0280....	1992 May 07 - May 14 ⇒	$< 6.0 \times 10^{-8}$	(a)	...	...		1992 Apr 29	$F_{37} = 0.58 \pm 0.13$
0370....	1992 Aug 20 - Aug 27			1992 Aug 28	0.94 ± 0.03	(b)	1992 May 06	$F_{14.5} = 0.33 \pm 0.01$
...	...	...		...	...		1992 Sep 01	$F_{22} = 0.94 \pm 0.03$
3170....	1994 Feb 17 - Mar 01			...	...		1994 Mar 15	$F_{22} = 0.78 \pm 0.11$
4250....	1995 Jul 25 - Aug 08 ⇒	$< 5.6 \times 10^{-8}$	(c)	...	...		1995 Jul 20	$F_{22} = 0.75 \pm 0.04$
...	...	...		...	...		1995 Aug 04	$F_{22} = 0.83 \pm 0.05$
...	...	...		...	...		1995 Aug 06	$F_{37} = 0.91 \pm 0.06$

Table 1 we summarize properties and available multiwavelength fluxes of GC 0109+224. The SED data profile in Fig. 7, points out a synchrotron peak in the frequency range around the near-infred, optical (and possibly near-UV) range. This strengthens the assumption that GC 0109+224 is an LBL or intermediate blazar, (as suggested for example in Laurent-Muehleisen et al. 1999; Dennett-Thorpe et al. 2000; Bondi et al. 2001).

Unfortunately, a part of one rather low EGRET upper limit, no data is available to check the presence of the inverse Compton (IC) emission bump (the few and old X-ray observations seems to have a synchrotron origin). The 1 keV flux, measured by ROSAT PSPC instrument in August 1990, is $F_X = 0.26 \pm 0.08 \mu$Jy, with $\alpha_X = 1.96 \pm 0.25$ (Table 1 and Fig. 7). This suggests a decreasing soft-X trend, in the νF_ν representation. The 1 keV flux by EXOSAT CMA instrument in August 1984, is approximately the same ($F_X = 0.21 \mu$Jy), while the 2keV flux by *Einstein* Observatory (HEAO-2) IPC and MPC instruments in July 1979, is $F_X = 0.15$ μJy. These detections seem to prove the highest energy synchrotron tail is emitted in the soft-X ray band (as is commonly found in intermediate blazars).

IRAS measured a flux density of 188 mJy at 60 μm and upper limits at the other its bands (Impey & Neugebauer 1988). As cited above GC 0109+224 seems characterized by a very strong (2-3 Jy) millimetre flux (a part of calibration uncertainties). On March 29, 2000, the IRAM Mambo bolometer measured a flux of 3.13 and 3.31 Jy at 1.2 mm (250 GHz), (and all other few available measurements are above 1 Jy, Bertoldi 2002). While on April 26, Metsähovi detected a flux above 2 Jy at 87 GHz (Fig. 2 and Tab. 1). No simultaneous optical data were available during this period in which the source is not visible on night, but February 2000 observations suggest a relevant high emission state (F$_\nu$(0.44 μm)$\simeq$ 16 mJy). According to (Valtaoja & Teräsranta 1996; Jorstad et al. 2001), γ-ray flares are considered connected to the rising or high state of the blazar millimetre emission. GC 0109+224 seems on a rising phase during September 1992 as showed by the radio flux curves, but it was not detected in γ-rays by EGRET. This could contradict the cited hypothesis, or the γ-rays were of short duration, or again probably the sensitivity was inadequate. The integral flux density upper limit (u.l.) above 100 MeV is rather low: the limit given in the first EGRET catalog (phase 1, Apr. 1991 - Nov. 1992) is $F_\gamma < 6 \times 10^{-8}$ photons cm^{-2} s^{-1}, approximatively equivalent to 1 nJy. The low optical brightness and the small radio fluxes (sub-Jansky), reported in Table 2, in correspondence with the EGRET viewing periods, point out a low or, in any case, non-flaring states. For details on the EGRET viewing periods pertaining to GC 0109+224, and corresponding available optical and radio fluxes, see Table 2.

We tentatively fitted the few available data with a pure one-zone homogeneous leptonic SSC model, in two representatives (low and high) states of the source (continuous lines in Fig. 7 for the August-October 1990 quiescent state, and the December 2000 flaring state). The multiwavelength SED data are grouped in epochs in Fig. 7 (but we remark that this is only a rough incongruent and temporally broad regroupment of the data). The applied model assumes a blob of dimension R embedded in a tangled isotropic magnetic field of mean intensity B, subjected to a continuous injection of shocked relativistic electrons with a break power law energy distribution, exponentially damped: $Q_{inj}(\gamma) = Q_0 \gamma^{-p} \exp(-\gamma/(k\gamma_{max}))$ [cm^{-3} s^{-1}], between the energies (Lorentz factors) γ_{min} and γ_{max}. This emitting region moves in a relativistic jet, approximatively aligned with our line of sight and fed by an accreting supermassive black hole. The mechanism is described using a one–dimensional and time–dependent kinetic equation for the electron particle distribution, and the ensemble synchrotron spectrum is convolved with the calculated distribution. The IC spectrum results from the interaction of the distribution with the synchrotron photon field. The produced spectra were transformed to the frame of the observer (placed at an angle θ respect to jet direction), using the relativistic Doppler beaming bulk factor $\mathcal{D} = ((1+z)\Gamma(1-\beta\cos\theta))^{-1}$. The model is described for example in (Ciprini & Tosti 2003c; Ciprini 2003d). The values of the parameters adopted for the two SED parameterisation of GC 0109+224, are reported in the figures caption. The steep injection ($p > 2$) and the exponential damping, creates a few high energy electrons (important for the IC emission). Moreover the relatively high value of B (0.45-1.6 G), means a stronger magnetic field energy density $U_B = B^2/(8\pi)$, and a smaller radiation to magnetic energy ratio $U_{rad}/U_B = L_{IC}/L_{syn}$, redicing the self-Compton flux.

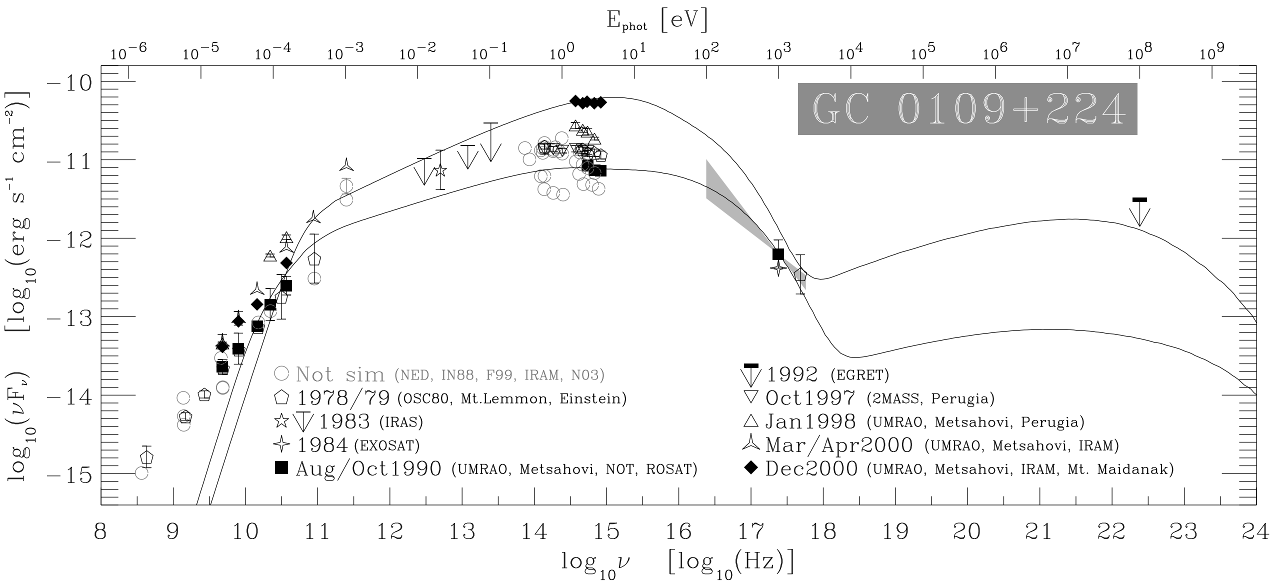

Figure 7. The SED of GC 0109+224 assembled with the available multiwavelength data (open and filled symbols), upper limits (arrows), and ROSAT slope (bow-tie), at different epochs. Two SSC model fit attempts (black lines) are used, for a low emission state and an high state. The SED is consistent with a pure smooth synchrotron continuum, peaking between the near-IR, optical, near-UV, range. EGRET upper limit above 100 MeV is rather low. There is no evidence of gamma-ray emission bump, and the few X-ray detections suggests a downward trend. Data are grouped for no-simultaneous epochs with the same symbol. Instruments or references are indicate in parentheses. Data from this work (UMRAO, Metsähovi and Perugia observatories), NED database, from (Owen et al. 1980, OSC80), Mt. Lemmon (Puschell & Stein 1980), from (Fan 1999, F99) and (Nesci et al. 2003, N03), Einstein IPC (Owen et al. 1981; Ledden & Odell 1985), IRAS (Impey & Neugebauer 1988, IN88), EXOSAT CMA (Maraschi & Maccagni 1988; Giommi et al. 1990; Reynolds et al. 1999), NOT (Valtaoja et al. 1993), ROSAT PSPC (Neumann et al. 1994; Brinkmann et al. 1995; Kock et al. 1996; Reich et al. 2000), EGRET (Fichtel et al. 1994; Hartman et al. 1999), 2MASS (Skrutskie et al. 1997), IRAM Mambo (Mar00, Jan01 and Jan02, Bertoldi 2002) and Mt. Maidanak (Ciprini et al. 2003a). The two lines referring to the SSC fit attempts for the flaring state of December 2000 and the low state around the ROSAT detection on 1990, are performed with the following parameters. **August/October 1990 low state**: $\gamma_{min} = 60$, $\gamma_{max} = 1.7 \times 10^6$, $\gamma_{break} = 5 \times 10^3$, $p_1 = 2.4$, $p_2 = 2.5$, $k = 0.015$, $B = 0.45$Gauss, $R = 9.5 \times 10^{16}$cm, $\mathcal{D} = 13$. **December 2000 high state**: $\gamma_{min} = 20$, $\gamma_{max} = 5 \times 10^5$, $\gamma_{break} = 7 \times 10^3$, $p_1 = 2.1$, $p_2 = 2.2$, $k = 0.015$, $B = 1.6$Gauss, $R = 8.5 \times 10^{16}$cm, $\mathcal{D} = 15$. Redshift $z = 0.4$ is assumed (Falomo 1996).

Indeed in our modelling (Fig. 7) the IC component appears depressed. The few multiwavelegth data available do not contain any hint of an high-energy spectral component. The values used for the physical parameters partially take in account radio flux data in the SED. For example lower values of γ_{min} could fit better the lower frequency radio data, but the IC emission is further depressed. The synchrotron spectral shape indicated by the available data, appears also to be suitable for a fit with logarithmic parabolic functions (see, e.g. Giommi et al. 2002; Sambruna et al. 1996). Probably, as stated for the flux curves, the dynamics and the regions involved in the high energy emission are different from the radio ones. Anyway the usual neglect of the radio data points in blazar SED modelling is not ever justified.

SED data and modelling (Fig. 7), allude to a synchrotron peak ranging between the near-IR, for the quiescent states, and the optical (perhaps also near-UV) bands for the flaring states. This is consistent with the view of GC 0109+224, as a blazar at the border of the LBL and intermediate subclasses. As a classical BL Lac, the SED is represented well with our pure leptonic SSC model. Therefore, with simple scaling considerations, the IC emission can be seen as the synchrotron component upshifted by γ_{max}^2 (with $\gamma_{max} \simeq 10^5$ in this case). The peak in the optical, in SSC descriptions, can predict a possible IC peak in GeV γ-ray energies through the following similarity relation: $(\nu_{GeV} F_{GeV})/L_{IC} \simeq (\nu_{opt} F_{opt})/L_{syn}$, (as the the synchrotron X-ray end tail is related to the TeV γ-ray tail in the HBLs (Stecker et al. 1996)). L_{syn} and magnetic fields intensity might be high for this object, reducing the IC dominance. However the strong millimeter flux, the peak of the SED in near-IR-optical bands, and the brightness in X-ray frequencies, might suggest the possibility of γ-ray emission. This emission may be detectable by the next generation of γ-ray satellites with improved sensitivity (e.g. AGILE and GLAST). Moreover we note the possible correlation of GC 0109+224 with one of the highest energy cosmic-rays events ever detected, $E = (1.7 - 2.6) \times 10^{20}$eV, on Dec. 3, 1993 (Farrar & Biermann 1998). In the scenario evading the GZK-cutoff, the primaries produced by particle acceleration in a blazar, should travel extragalactic distances not deflected, pointing directly to its source, and under this assumption the probability of a coincidental alignment of that event with GC 0109+224 was only 0.5% (Farrar & Biermann 1998).

5 SUMMARY AND CONCLUSIONS

In this work we have reported and analysed the largest amount of radio and optical data ever published on the BL Lac object GC 0109+224, collected over more than twenty years, and we have reconstructed also the most complete multiwavelength SED available. Some results are found, but

also open questions are arisen. GC 0109+224 is an example of a blazar which can produce strong outburst at high radio frequencies (2-3 Jy at $\nu \gtrsim 20$ GHz), but can remain relatively quiet ($\simeq 0.3$Jy GB6 survey) for long periods. The flux density variability is characterized by intermittent behaviour, with a not regular alternation of relatively large amplitude flares, and flickering phases, both in radio and optical regimes. The source varies over all timescales sampled (days, months, years). Optical flares are clearly much faster with respect to the radio-mm bands, and some particularly large optical outbursts do not have obvious counterparts at mm and radio wavelengths. This could suggest additional or different emitting components responsible for the radio and the optical emission, and/or more rapid cooling of the synchrotron particles at higher frequencies. Moreover radio flares, due to the longer duty cycles, can blend, inhibiting the identification of radio counterparts of the optical flares.

The radio light curves appear well correlated at the different frequencies, around the zero lag. The radio–optical cross–correlation peaks, found in all the bands around the lag of 2.1-2.4 years, are extended and have low values (ZDCCF < 0.62). The complexity, spread and low values of the correlation peaks, the impossibility to visually recognize the lags in the light curves, the very different duty-cycles, and especially such long delays, suggest that there is not a real correlation, and no physical meaning in the two-year lag. Other shorter delays around 33, 190, and 500 days are not significant because they are found with very small correlation coefficients. Fig. 3 shows also that the signal is weak at zero time lag (between optical and 37-22 GHz curves). This means that strong events in the optical bands do not have a simultaneous recognizable counterpart in the radio bands. Maybe additional processes and/or different regions are responsible for the emission at different frequencies (optical photons could be generated into jet components of different size and dynamics, in correspondence to the radio emission). A certain level of confusion is undoubtedly created by induced causes (i.e. the large empty gaps in the optical light curve data). Only with continuous monitoring over longer periods, with reduced gaps, will clarify the existence of physical radio–optical delays in this source.

The DCF and SF shapes reflect the underlying nature of the process that created the radio variability. Both methods demonstrate, for GC 0109+224, a fluctuation mode between the flickering and the shot noise (i.e. $P(f) \propto 1/f^{\alpha}$), with $1.39 < \alpha < 1.65$. A similar behaviour was found also for the optical emission (Ciprini et al. 2003a,b) of this source. This power spectrum is characteristic of a random walk. In the case of the best sampled 22 GHz light curve, the value $\alpha = 1.65$ found, is in strict agreement with the 5/3 value of the fully develop turbulence in the scalar theory of Kolmogorov. Such variability could be related to fluctuations of the magnetic field, or of the bulk motion velocity of the emitting regions inside the jet.

There is no evidence from our data, for long term periodic variations with a fixed period, but typical timescales in the ranges of $\sim 3.2 - 4.5$ years are implied, with all the applied methods (DCF, SF, periodogram). The more rapid flickering synchrotron peaks, seem superimposed to long term trends in the radio. This could also be the result of flares blending with long cooling times, as mentioned above.

The increased activity and mean flux level, well observed in all the radio–optical bands, suggest that the same emission mechanism is responsible for radiation in both spectral regimes, i.e. the synchrotron radiation from shocked plasma into the jet, as seen also in the SED. Synchrotron emission in GC 0109+224 is probably dominant and powerful ($L_{syn}/L_{IC} > 1$), as suggested by the high degree of the polarization, and by the absence of emission lines (z is still undetermined). The relatively high degree of linear polarization observed could mean a weaker connection with the usual depolarization effects, which is a common affliction of blazars jets (like influence of a luminous host galaxy). The overall SED of GC 0109+224, shows a smooth synchrotron continuum peaked in the near-IR-optical range (as showed by intermediate blazars). Also our homogeneous SSC modelling suggests a relatively high magnetic field and synchrotron luminosity, diminishing the self-Compton radiation, even thought the multiwavelength data reported are insufficient to fully constrain the models. In particular GC 0109+224, suffers from substantial lack of data in millimetre sub-mm and infrared bands, to check the importance of a possible thermal emission component (and also the possibility of external-Compton contributions).

Despite of the common deficiency of infrared data, and difficulties for far and mid-IR blazar monitoring, we suggest at least millimetre observations, due to the intense radiation which GC 0109+224 seems produce at these frequencies. X-ray observations of this blazar are also strongly encouraged, to check the presence of the high energy component in the spectrum. The high energy predictions for an intermediate blazar suffer uncertainties that become relevant in high energy tails, even when only using leptonic models (Böttcher et al. 2002). Moreover the X-ray data are insufficient to permit any prediction about TeV gamma-rays from this object (due to the suggested $z > 0.4$, TeV emission might be interesting for studies on the extragalactic background light by absorption cutoffs). However millimetre brightness, and synchrotron emission peaked at optical frequencies, could imply a GeV gamma-ray radiation detectable by the next-generation of gamma-ray space telescopes. An increased observing effort for this source, especially at X-ray bands and beyond (for example GC 0109+224 is just scheduled to be observed by Integral Pian 2002)), together with a better monitoring in radio-mm-optical bands, will clarify some of the questions that have arisen in our data and analysis. In this view our data and work will be useful database.

6 ACKNOWLEDGMENTS

We wish to thank Kyle Augustson for useful comments. The Metshovi Radio Observatory is an institute of the Helsinki University of Technology, partially financed by the Academy of Finland. The UMRAO is supported by the US National Science Foundation, and by funds from the University of Michigan. The optical monitoring program of the Perugia University Observatory was partly supported by the Italian MIUR under grant Cofin2002. The European Institutes belonging also to the ENIGMA collaboration acknowledge EC funding under contract HPRN-CT-2002-00321. This research has made use also of: SIMBAD database (CDS,

Strasbourg), NASA/IPAC NED database (JPL CalTech and NASA), HEASARC database (LHEA NASA/GSFC and SAO), NASA's ADS digital library.

REFERENCES

Alexander, T. 1997, in Astronomical Time Series, Eds. Maoz, Sternberg & Leibowitz, Dordrecht: Kluwer, p. 163

Aller, M. F., Aller, H. D., Hughes, P. A., & Latimer G. E. 1999, ApJ, 512, 601

Aller, H. D., Aller, M. F., & Hughes, P. A. 1996, in ASP Conf. Ser. 110: Blazar Continuum Variability, p. 208

Bertoldi, F., 2002, private communication

Brinkmann, W., Siebert, J., Reich, W., et al. 1995, A&AS, 109, 147

Böttcher, M., Mukherjee, R., & Reimer, A. 2002, ApJ, 581, 143

Bondi, M., Marchã, M. J. M., Dallacasa, D., & Stanghellini, C. 2001, MNRAS, 325, 1109

Ciprini, S., Tosti, G., Raiteri et al. 2003a, A&A, 400, 487

Ciprini, S., Fiorucci, M., Tosti G., & Marchili, N. 2003b, ASP Conf. Series, 299, 265

Ciprini S., & Tosti G. 2003c, ASP Conf. Series, 299, 269

Ciprini, S. 2003d, New Astronomy Rev., 47, 709

Della Ceca, R., Palumbo, G. G. C., Persic, M., et al. 1990, ApJS, 72, 471

Dennett-Thorpe, J., & Marchã, M. J. 2000, A&A, 361, 480

Douglas, J. N., Bash, F. N., Bozyan, F. A., Torrence, G. W., & Wolfe, C. 1996, AJ, 111, 1945

Edelson, R. A., & Krolik, J. H. 1988, ApJ, 333, 646

Falomo, R. 1996, MNRAS, 283, 241

Fan, J. H. 1999, astro-ph/9910269

Farrar, G. R., & Biermann, P. L. 1998, Phys. Rev. Lett., 81, 3579

Fey, A. L., & Charlot P. 2000, ApJS, 128, 17

Fichtel, C. E., Bertsch, D. L., Chiang, J., et al. 1994, ApJS, 94, 551

Gaskell, C. M. & Peterson, B. M. 1987, ApJS, 65, 1

Giommi, P. et al. 2002, in Blazar Astroph. with BeppoSAX & Other Obs., ASI spec. publ., Rome, p. 63

Giommi, P., Barr, P., Garilli, B., Maccagni, D., & Pollock, A. M. T., 1990, ApJ, 356, 432

Hanski, M.T̃., Takalo, L.Õ., & Valtaoja, E. 2002, A&A, 394, 17

Hartman, R. C., Bertsch, D. L., Bloom, S. D., et al. 1999, ApJS, 123, 79

Horne, J. H., & Baliunas, S. L. 1986, ApJ, 302, 757

Hufnagel, B. R., & Bregman, J. N. 1992, ApJ, 386, 473

Hughes, P. A., Aller, H. D., & Aller, M. F. 1992, ApJ, 396, 469

Impey, C. D. & Neugebauer, G. 1988, AJ, 95, 307

Jorstad, S. G., Marscher, A. P., Mattox, J. R., Aller, M. F., Aller, H. D., Wehrle, A. E., & Bloom, S. D. 2001, ApJ, 556, 738

Kock, A., Meisenheimer, K., Brinkmann, W., Neumann, M., & Siebert, J. 1996, A&A, 307, 745

Laurent-Muehleisen, S. A., Kollgaard, R. I., Feigelson, E. D., Brinkmann, W., & Siebert, J. 1999, ApJ, 525, 127

Ledden, J. E., & Odell, S. L. 1985, ApJ, 298, 630

Maraschi, L., & Maccagni, D., 1988, MemSAIt, 59, 277

Maraschi, L., Ghisellini, G., Tanzi, E. G., & Treves, A. 1986, ApJ, 310, 325

Marchã, M. J. M., Browne, I. W. A., Impey, C. D., & Smith, P. S. 1996, MNRAS, 281, 425

Mead, A. R. G., Ballard, K. R., Brand, P. W. J. L., Hough, J. H., Brindle, C., & Bailey, J. A. 1990, A&AS, 83, 183

Nesci, R., Sclavi, S., Maesano, et al. 2003, MemSAIt, 74, 169

Neumann, M., Reich, W., Fürst, E., et al. 1994, A&AS, 106, 303

Odell, S. L.; Puschell, J. J.; Stein, W. A., et al 1978, ApJ, 224, 22

Owen, F. N., & Mufson, S. L. 1977, AJ, 82, 776

Owen, F. N., Helfand, D. J., & Spangler, S. R. 1981, ApJ, 250, 550

Owen, F. N., Spanger, S. R., & Cotton, W. D. 1980, AJ, 85, 351

Padovani, P. & Giommi, P. 1995, ApJ, 444, 567

Pauliny-Toth, I. I. K., Kellermann, K. I., Davis, M. M., Fomalont, E. B., & Shaffer, D. B. 1972, AJ, 77, 265

Pian, E. 2002, Blazar TOO, Integral Ann. of Opp. (AO-1)

Press, W. H., & Rybicki, G. B. 1989, ApJ, 338, 277

Puschell, J. J., & Stein, W. A. 1980, ApJ, 237, 331

Reich, W., Fuerst, E., Reich, P., et al. 2000, A&A, 363, 141

Reynolds, A. P., Parmar, A. N., Hakala, P. J., et al. 1999, A&AS, 134, 287

Sambruna, R. M., Maraschi, L., & Urry, C. M. 1996, ApJ, 463, 444

Scargle, J. D. 1982, ApJ, 263, 835

Simonetti, J. H., Cordes, J. M., & Heeschen, D. S. 1985, ApJ, 296, 46

Sitko, M. L., Schmidt, G. D., & Stein, W. A. 1985, ApJS, 59, 323

Skrutskie, M. F., Schneider, S. E., Stiening, R., et. al. 1997, ASSL Vol. 210, Dordrecht: Kluwer, p. 25

Stecker, F. W., de Jager, O. C., & Salamon, M. H. 1996, ApJ, 473, L75

Tagliaferri G., Ghisellini G., Giommi P. et al. 2000, A&A, 354, 431

Takalo, L. O. 1991, A&AS, 90, 161

Teräsranta, H., 2002, in Blazar Astroph. BeppoSAX & Other Obs., ASI Special Publ., Rome 2002, p. 215

Teräsranta, H., Tornikoski, M., Mujunen, A., et al. 1998, A&AS, 132, 305

Thompson, D. J., Bertsch, D. L., Dingus, B. L., et al. 1995, ApJS, 101, 259

Tosti, G., Massaro, E., Nesci, R., Ciprini, S., et al. 2002, A&A, 395, 11

Tosti, G,, Pascolini, S., & Fiorucci, M. 1996, PASP, 108, 706

Valtaoja, E. & Teräsranta, H. 1996, A&AS, 120, 491

Valtaoja, L., Karttunen, H., Efimov, Y. S., & Shakhovskoy, N. M. 1993, A&A, 278, 371

Valtaoja, L., Sillanpää, A., Valtaoja, E., Shakhovskoi, N. M., & Efimov, I. S. 1991, AJ, 101, 78

Wilkinson, P. N., Browne, I. W. A., Patnaik, A. R., Wrobel, J. M., & Sorathia, B. 1998, MNRAS, 300, 790

Wright, S. C., McHardy, I. M., Abraham, R. G., et al. 1998, MNRAS, 296, 961

Zacharias, N., Zacharias, M. I., Hall, D. M. et al. 1999, AJ, 118, 2511